01 Jun 1988, 1:00 pm - 5:30 pm

Stability Analysis of Seismically Damaged Embankments

Yasuyuki Koga
Public Works Research Institute, Ministry of Construction, Japan

Osamu Matsuo
Public Works Research Institute, Ministry of Construction, Japan

Proceedings: Second International Conference on Case Histories in Geotechnical Engineering, June 1-5, 1988, St. Louis, Mo., Paper No. 4.01

Stability Analysis of Seismically Damaged Embankments

Yasuyuki Koga
Head, Soil Dynamics Division, Public Works Research Institute, Ministry of Construction, Japan

Osamu Matsuo
Senior Research Engineer, Soil Dynamics Division, Public Works Research Institute, Ministry of Construction, Japan

Synposis: This paper describes a pseudo-static stability analysis of seismically damaged embankments during the 1983 Nihonkai-chubu earthquake (Japan). It places a great emphasis on the discussion of a dynamic shear strength of soils to be used in a seismic stability analysis of embankments.
Several existing concepts of a dynamic strength are reviewed, which vary from each other with respect to loading patterns, drainage conditions and strength criteria in soil element tests. The main part of this paper is to apply some of the dynamic soil strengths discussed above to seismic stability analyses of three embankment sections, laid on loose sandy deposits which were damaged by the 1983 Nihonkai-chubu earthquake in Japan, and to evaluate the applicability of those strengths. Dynamic response analyses and pseudo-static stability analyses were performed on the basis of field and laboratory soil test data, such as SPT, shear wave logging, CPT, VCPT (vibratory cone penetration test) and cyclic triaxial compression test. The safety factors obtained from the analyses were compared with the settlements of respective embankment sections which would have possibly occurred during the earthquake. It was concluded that the dynamic shear strength, which is defined as a sum of static and dynamic shear stresses that can produce a certain value of cumulative shear strain in a certain number of stress cycles, is the most reasonable of them.

INTRODUCTION

It is widely recognized that the knowledge of a dynamic strength of soils is essential for a seismic stability analysis of slopes and embankments. They have been studied to date in a number of case studies and their concepts have already been described in some of the related design guidelines for practice.

However, the applicability of each concept of a soil strength for a seismic stability analysis has not yet been clearly discussed. This paper first reviews and discusses existing several types of soil strengths for seismic stability analyses and their premises as well.

Secondly three types of strengths of those above are applied to seismic stability analysis of three embankment sections which were damaged due to liquefied foundations in the 1983 Nihonkai-chubu earthquake in Japan. Then a rational soil strength for a seismic stability analysis is deduded on the basis of the comparison of the analyzed results and damage records in the field.

CONSIDERATION ON A DYNAMIC SHEAR STRENGTH OF SOILS FOR SEISMIC STABILITY ANALYSIS

Failure of slopes and embankments due to earthquakes

Damages to slopes and embankments are often observed after a large earthquake. Such failure phenomena can be classified as follows from the viewpoint of a seismic motion and a time of failure occurrence.

1) Failure during an earthquake: this is most usually called a failure due to an earthquake and actually occurs most frequently.

2) Failure relatively soon after an earthquake ends: this sometimes occurs without such a change of an external load as rainfall after the load condition returns to a pre-earthquake condition. This requires a decrease of the resistance of embankment and ground, which is reduced to the change of an excess pore pressure distribution caused by a seismic load in the previous earthquake. This also belongs to the failure due to an earthquake and can be called as failure after an earthquake more

literally.

3) Some slopes where cracks have occurred during an earthquake fail fairly after an earthquake with the aid of rainfall and other causes. This may be included in the failure due to earthquake in a broad sense, however, this is generally excluded.

Such a classification plays an important role in a consideration of a load and a shear strength of soils for a seismic stability analysis.

Seismic stability analysis method

Though several analytical methods are available to investigate the stability of slopes, the simplest is a slip surface stability analysis based on a limit equilibrium method.

The effect of a seismic motion is considered as a static force through a seismic coefficient in a seismic stability analysis. Calculation formula for a slip surface analysis is given by

$$F_s = f\ (W,\ \tau_f,\ k\ ) \qquad (1)$$

where, F_s = a safety factor, f = a calculation equation of a safety factor, W = soil weight, τ_f = strength of a soil and k = a seismic coefficient.

Eq. (1) shows a close interdependence of the factors. Therefore it is necessary to pursue a harmonized analysis method considering the interdependence of the factors. When a seismic effect is converted to a static force, seismic stability analysis equations can easily be obtained extending various static stability analysis equations.

Shear strength of soils for seismic stability analysis method

As is already described, slope failures due to earthquakes can be classified into failure during and after earthquakes respectively.

A shear strength of a soil is usually obtained by loading soil specimens in such a manner as will occur in the actual condition. Therefore each loading manner for the failure during and after an earthquake is as follows.

Failure during an earthquake : the strength σ_f is obtained from the condition for the strain to reach failure strain ε_f by changing the dynamic stress amplitude σ_d to correspond with a seismic inertia force.

Failure after an earthquake : As the load basically returns to an original one when an earthquake ends, the slope which did not fail during an earthquake, cannot fail, if its individual part behaves independently. Therefore the slope which actually failed should be reduced to the phenomenon in the overall slope such as a redistribution of the stress due to creep phenomenon and the pore pressure due to seepage. However, the residual strength σ_f against a static load after the soil was subjected to a static and a dynamic stress due to dead weight and a seismic motion may be used as a reference strength in this case.

The latter strength can also be used for a seismic stability analysis during an earthquake as follows. Consider a state of a slope which was subjected to N cycles of a dynamic stress to analyze a stability during an earthquake, then a safety factor can be obtained by comparing the dynamic stress of the next N + 1 th cycle and the residual strength after N cycles of stress.

Table 1 is a summary of the above statement. Also is summarized in Table 2 various shear strengths of a soil for a seismic stability analysis. Here a saturated soil under undrained condition is considered. Figs. 1 and 2 show assumed loading patterns for respective strengths and stress paths to reach a failure. In Table 2 six types of strength are classified into static and dynamic ones.

Table 1 Loading patterns for respective types of failure

Failure during an earthquake	**loading pattern: Fig. 1 or Fig. 2**
Failure after an earthquake	**loading pattern: Fig. 2**

A static strength is mobilized under a monotonous loading as shown in Fig.1 (a) and used as an approximation of a dynamic strength for a seismic stability analysis. A dynamic strength assumes a repetitive loading as shown in Figs. 1 (b) (c). These are used for a stability analysis during and after an earthquake respectively. Moreover the latter dynamic strength can also be used for a stabi- lity analysis during an earthquake as stated previously. Among the six types of strengths, the features of three strengths (strength A, C, D) being frequently used in practice for a seismic stability analysis of embankments are as follows.

Table 2 Classification of strength

Type	Strength criteria	Drainage condition	Loading pattern	Stress path & strength	Time of strength mobilized	Corresponding loading condition	Reference**)
Static strength (Monotonous loading)	Mobilized maximum stress under a monotonous loading	Drained	a	A	during earthquake (high permeability)	Dead weight + seismic force	JNCOLD (1978)
		Undrained	a	B, B'	during earthquake (impulsive earthquake)	do	do
Dynamic strength (Cyclic loading)	Maximum stress of stress time history to cause a reference strain during a cyclic loading	Undrained	b	C	during earthquake	do	Seed (1966) Ishihara (1980)
	Maximum static strength after a cyclic loading	Incompletely drained*) (Pore pressure during a cyclic loading remains constant)	c	D	during earthquake & soon after earthquake	do Dead weight	JNR (1972) PWRI (1975) HUDC (1984) JMA (1980)
		Undrained*)	c	E	during earthquake & soon after earthquake	Dead weight + Seismic force Dead weight	Castro (1976) Seed (1979) Tokyo Metro. Govnt. (1983) Seed (1979)
		Drained*) (Pore pressure returns to initial pressure)	c	F	long after earthquake	do	

N.B. *) This drainage condition refers to that for a static loading after a cyclic loading.
An undrained condition is assumed during a cyclic loading.

Fig.3 shows the relation between above three strengths and number of cycles of seismic load for a saturated sand for which respective strengths differ very much. Here the strengths are expressed as follows.

$$\text{Strength A} : \tau_f = \bar{\sigma}_{no} \cdot \tan \phi' \quad (2)$$

$$\text{Strength C} : \tau_f = \bar{\sigma}_{no} \cdot \tan \phi_D = \bar{\sigma}_{no} \cdot R_\ell(N) \quad (3)$$

$$\text{Strength D} : \tau_f = (\bar{\sigma}_{no} - u_e) \cdot \tan \phi' = \bar{\sigma}_{no} \cdot (1 - u_e/\bar{\sigma}_{no}) \cdot \tan \phi' \quad (4)$$

where τ_f = shear strength, $\bar{\sigma}_{no}$ = initial effective normal stress, ϕ' = angle of static shearing resistance, ϕ_D = angle of dynamic shearing resistance, R_ℓ (N) = liquefaction strength ratio, u_e = excess pore pressure caused by a cyclic loading.

The strength A is a constant being independent of external load.

The strength C is deter- mined if the equivalent number of cycles Neq of a seismic load and a failure strain γ_f are given.

The strength D depends on a stress τ_d and number of cycles Neq of a seismic load.

This indicates that the seismic effect up to a certain time has already been taken into account as an action to

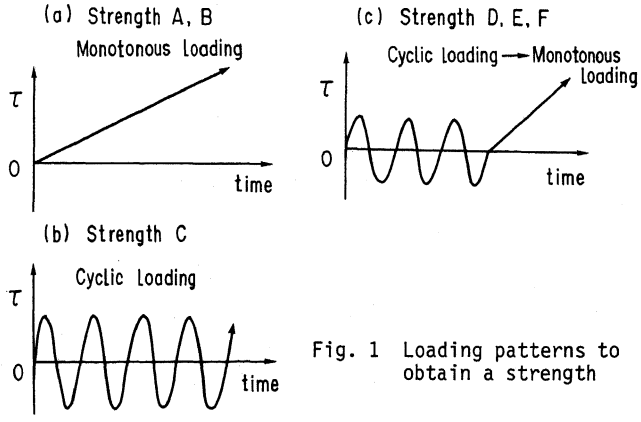

Fig. 1 Loading patterns to obtain a strength

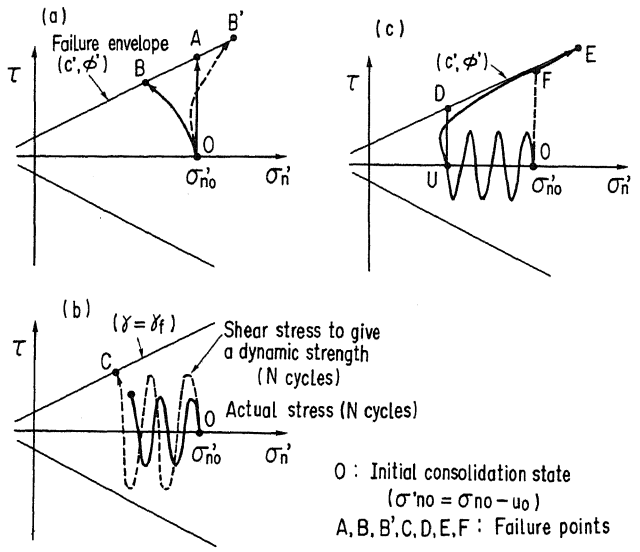

Fig. 2 Stress paths and strengths

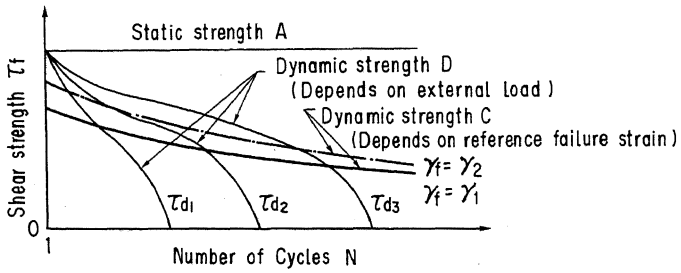

Fig. 3 Comparison of each strength

generate an excess pore pressure, therefore it is irrational if this strength is compared with the seismic load prior to that time to calculate a safety factor. Moreover it should be noted that the strength D is a post-earthquake strength under a special drain condition. Consequently these strengths can have a remarkable difference.

OUTLINE OF DAMAGED EMBANKMENTS

The 1983 Nihonkai-chubu Earthquake

The Nihonkai-chubu earthquake whose epicenter was in Japan Sea hit the northern part of Honshu-Island, Japan, on May 13, 1983 (Fig.4). Its magnitude was 7.7 in the Richter scale. The characteristics of the damage by this earthquake was the failure of many earth structures such as river dykes and road embankments which was mainly caused by the liquefaction of the sandy ground.

Outline of analyzed embankments

Among the damaged river dykes, Hachirogata reclamation

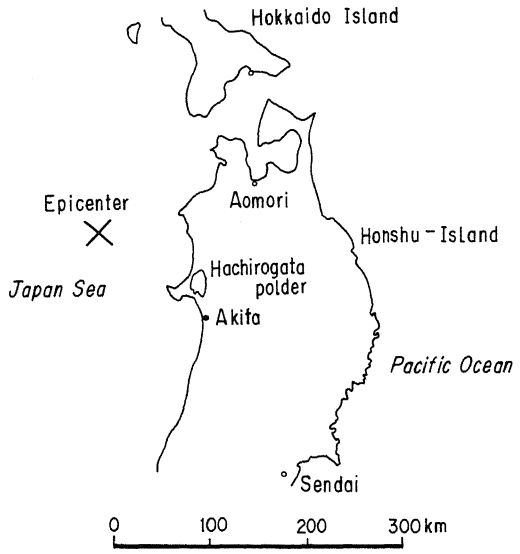

Fig. 4 Location of analyzed embankment sites

dyke which encloses a reclaimed land with the length of 100 km were damaged around 70 % of its total length. Three sections of this reclamation dyke which were located within 200 m were chosen for a detailed seismic analysis. These three sections showed a fairly different settlements as shown in Table 3 with a height of about 4.6 m. Because of such a difference, a rather detailed soil exploration and an analysis were conducted.

Table 3 Crest settlement of each section

Site A	19 cm
Site B	73 cm
Site C	133 cm

Soil exploration

The conducted items of soil exploration are summarized in Table 4. Besides conventional soil test items, some dynamic soil exploration and tests were conducted as shown in the Table. The VCPT (Vibratory Cone Penetration Test) was developed at the PWRI to assess the liquefaction strength of sandy ground. Cyclic triaxial tests of undisturbed samples were performed to obtain conventional liquefaction strength R_ℓ and dynamic strength under initial static shear stress based on a cumulative strain by use of isotropically consolidated and anisotropically consolidated specimens respectively. Fig. 5 shows the soil profiles obtained from above soil exploration. However, the number of undisturbed soil samples were not enough to conduct cyclic triaxial tests under all the required stress conditions. Therefore the effect of initial shear stress condition on a dynamic strength was

Table 4 Items of soil exploration

Item \ Site		Akita port	A	B	C
Soil exploration	SPT (depth, m)	50.0 m	24.4 m	20.6 m	30.5 m 40.5 35.5 20.6
	Dutch cone test (length, No. of points)	—	—	—	32.2 m x 1 19.0 ,, 33.0 ,,
	VCPT*) (length, No. of points)	—	8.9 m	12.0 m	12.0 m
	Ram sounding (length, No. of points)	—	—	—	30.0 m x 3
	Seismic wave logging (length)	18 m	—	—	43 m
Dynamic soil laboratory test	Resonant column test (No. of specimens)	—	—	—	1
	Cyclic triaxial test (No. of specimens)				
	Isotropic consolidation	—	—	—	10
	Anisotropic consolidation	—	4	7	8

N.B. *): Vibratory Cone Penetration Test, developed at PWRI to assess a liquefaction strength at the field.

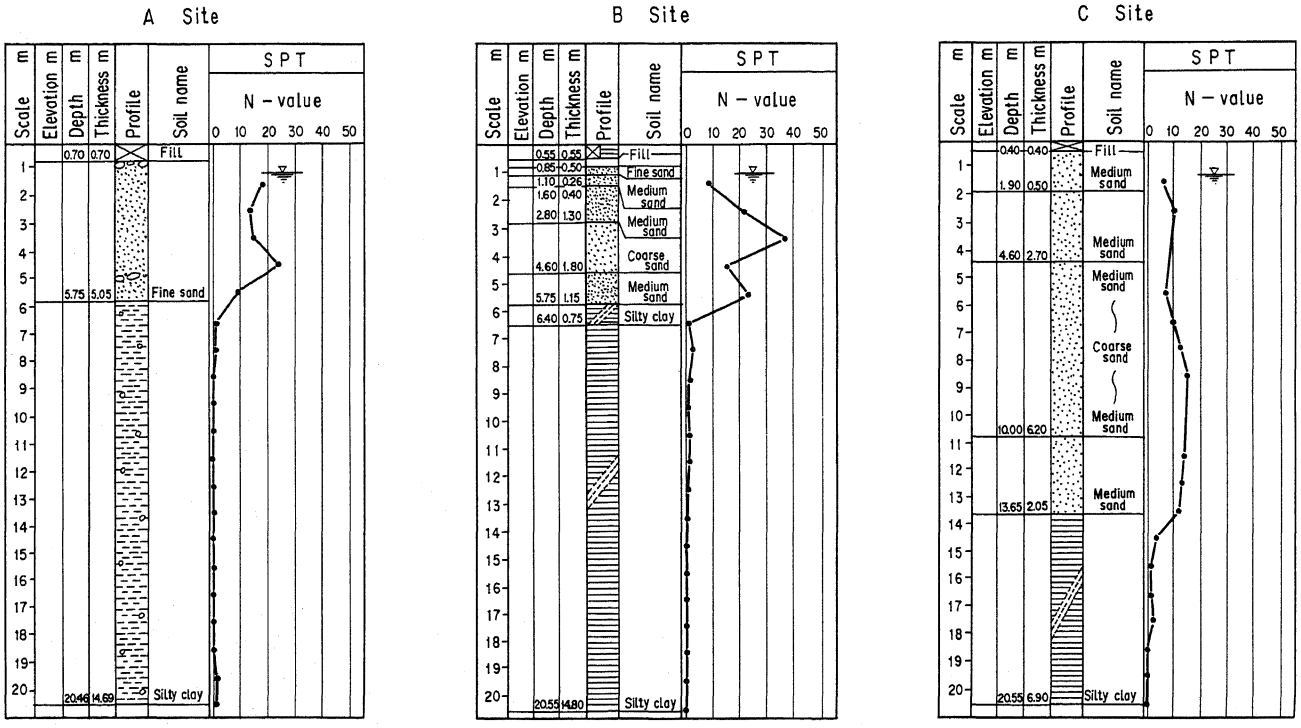

Fig. 5 Soil profile for each site

mainly assumed from existing data of another sand (Sengenyama sand) with similar gradation as this sand. Fig. 6 shows a main characteristic obtained in this manner. In this Figure, point A indicates a liquefaction strength R_ℓ without initial shear stress. The overall curve was vertically shifted to fit this point A to that of each site without changing the curve shape.

The characteristics of the excess pore pressure required to obtain a dynamic strength based on the excess pore pressure generated by a cyclic loading were obtained from cyclic triaxial tests of isotropically consolidated specimens. It is arranged as in Fig. 7.

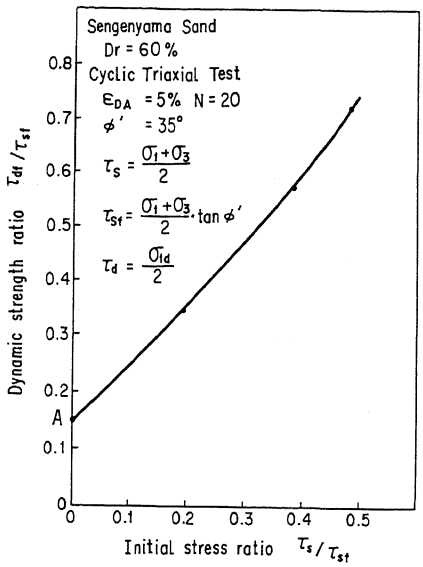

Fig. 6 Effect of initial shear stress on a dynamic strength

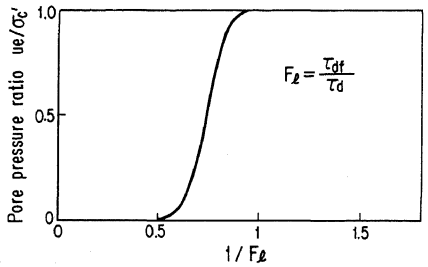

Fig. 7 Pore pressure generation chracteristics

SEISMIC STABILITY ANALYSIS

Dynamic response analysis and seismic coefficient

The seismic coefficient for a seismic stability analysis was obtained following the procedure shown in Fig. 8.

A seismic record at the Akita port of around 17 km distance from the analyzed embankment sites were utilized. The program SHAKE was used for the multiple reflection analysis to consider the nonlinear characteristics of soil layers as the equivalent linear ones. The diluvial sandy gravel layer was assumed as a bedrock for the analysis. The seismic response of the embankments was analyzed by the 2 dimensional FEM program SADAP developed at the PWRI to consider the nonlinear and hysteretic characteristics of soil layers by step-by-step numerical analysis. The equivalence coefficient C_r to convert a maximum acceleration response of the embankment a_{max} to a seismic coefficient K_h was calculated assuming the shear stress wave form is similar to that of the response acceleration and then

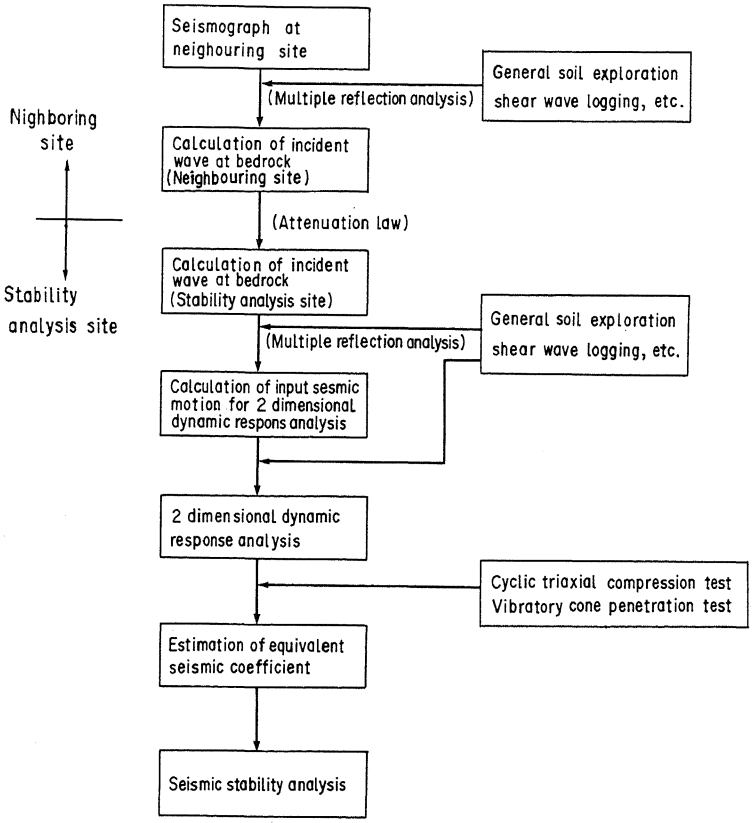

Fig. 8 Calculation of seismic coefficient

combining the cumulative damage concept and dynamic strength characteristics. Then an equivalent seismic coefficient K_h was calculated by the formula

$$K_h = C_r \times a_{max}/g \qquad (5)$$

which was used for a seismic stability analysis described in the next section. It is noteworthy that C_r depends on the reference number of loading cycles Neq. As Neq increases, C_r decreases. Assuming Neq = 20, C_r was obtained for each site as follows:

Site A: C_r = 0.678, Site B: C_r = 0.689,
Site C: C_r = 0.689.

Seismic stability analysis method

The formula for a stability analysis was the following modified Fellenius method considering a simple circular slip surface (Fig. 9).

$$F_s = \frac{\Sigma\{c' \cdot \ell + (w - u \cdot b)\cos\alpha \cdot \tan\phi'\}}{\Sigma(w \cdot R\sin\alpha + k_h w \cdot y)} \quad (6)$$

$$= \frac{R\Sigma\tau_f \cdot \ell}{\Sigma(w \cdot R\sin\alpha + k_h w \cdot y)} \quad (7)$$

where c, ϕ, τ_f : cohesion, angle of shearing resistance and strength of soils respectively, u : pore pressure, see Fig. 9 regarding other notations.

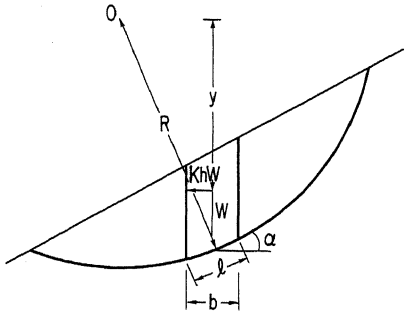

Fig. 9 Slip surface for seismic stability analysis

Three types of strengths described previously, that is, a static strength, a dynamic strength based on excess pore pressure during a cyclic loading and a dynamic strength based on a cumulative strain during a cyclic loading are considered. They are called as strength S_1, S_2, S_3 in the following. The conducted analysis cases are summarized in Table 5.

The strength S_1 was obtained assuming $c' = 0.1$ tf/m^2 and $\phi' = 35°$ in Eq. (6).

The strength S_2 can be obtained as follows. Calculate the stress ratio in the ground using the equivalent seismic coefficient k_h corresponding to N_{eq}=20. Then calculate excess pore pressure u_e through Fig. 7. The seismic stability analysis can be done substituting this u_e in Eq. (6). Considering that the maximum excess pore pressure may be generated during the seismic motion or after it ends, two cases of stability analyses with a seismic coefficient k_h (Case S_2) and without k_h (Case S_2') were conducted.

Table 5 Analysis Cases

Case	Strength parameters	Seismic coefficient	Pore pressure
S_1	$C' = 0.1$tf/m^2, $\phi' = 35°$	With	hydrostatic pressure
S_2	"	With	hydrostatic and excess pressure
S'_2	"	Without	do
S_3	C_D, ϕ_D or τ_{fD}	With	hydrostatic pressure

The strength S_3 was incorporated in a seismic stability analysis by the method described by Ishihara (Ishihara, 1980) as follows.

First a static safety factor F_s was calculated using a static strength τ_{sf} for a specified slip surface. Secondly, assuming the stress ratio is constant and equals to $1/F_s$ along a slip surface, the dynamic strength τ_{df} is obtained from Fig. 6.

Stability analysis results

Though the seismic coefficient at each site was already presumed, safety factors F_s for respective cases were calculated changing the seismic coefficient k_h 0-0.3 in order to grasp the effect of k_h on F_s. The stability analysis results are shown in Fig. 10. Fig. 10 indicates the safety factor F_s depends much on the strength used. As regards both cases S_2 and S_2', F_s decreases remarkably when k_h exceeds a certain value, which reflects that the excess fore pressure is very sensitive to the liquefaction resistance coefficient F_ℓ.

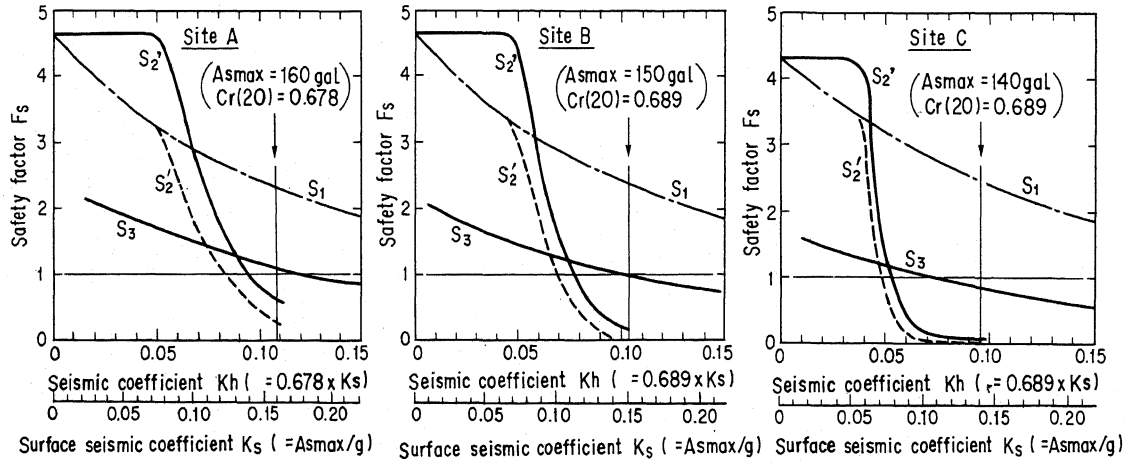

Fig. 10 Seismic coefficient vs. safety factor

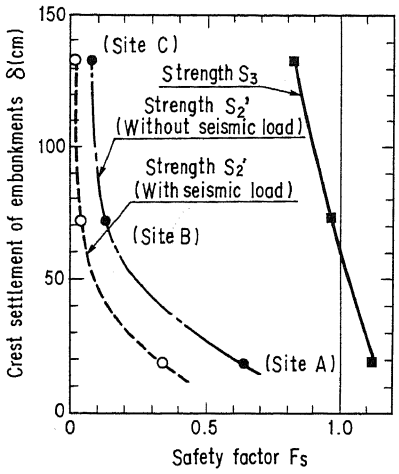

Fig. 11 Relation of safety factor vs. crest settlement

In the cases of S_1 and S_3, F_s changes depending only on the seismic coefficient k_h and its difference corresponds to the difference of the strength S_1 and S_3. Moreover, the estimated seismic coefficients are indicated in Fig. 10. The figure shows that the safety factors by use of the strength S_1 are fairly larger than unity, which contradicts the fact that each site was subjected to some damage. The relation between the safety factors using S_2, S_2', S_3 and the settlement of the embankments is plotted in Fig.11. All the relations appear reasonable in that the settlement is large when F_s is small, however, F_s is too small in the cases where S_2 and S_2' were used, considering the fact that some embankments in the neighborhood of these three were little damaged. Therefore these two strengths rather seem to lack rationality. On the other hand, in the case where S_3 was used, F_s equals to approximately 1.2 when some damage occurs and F_s does not extremely decrease when the settlement is large. The corresponding relation between the settlement and F_s seems comparatively reasonable.
This suggests that it is more rational to use a dynamic strength of a soil based on a cumulative strain for a seismic stability analysis (during an earthquake) than other strengths.

CONCLUSIONS

Several dynamic shear strengths of a soil to be used for a seismic stability analysis were reviewed. In the adoption of respective strengths, the correspondence of the time when the failure occurrs and the premise of the strength must be carefully noted. Three shear strengths of a soil frequently used in practice were compared on the basis of the analysis of damaged river embankments at the Nihonkai-chubu earthquake. They are a static strength, a dynamic strength based on cumulative strain during a cyclic loading and a dynamic strength calculated through an excess pore pressure during a cyclic loading. The analysis results showed the dynamic shear strength based on a cumulative strain gives a reasonable relation to reported settlement. This proved rationality of using a dynamic strength based on a cumulative strain for a stability analysis during an earthquake.

REFERENCE

Castro, G. and Christian, J.T. (1976), "Shear Strength of Soils and Cyclic Loading", Journ. of GED, Proc. ASCE, Vol. 102, No. GT9.
Housing & Urban Development Corporation, Urban Development Department (1984), "Technical Guideline for Earthquake Resistant Design of Housing Construction Site (draft)", (in Japanese).
Ishihara, K. (1980), "Current Practice and Problems in the Earthquake Resistant Design of Earth Structures", Tsuchi-to-Kiso, JSSMFE, 28-8, (in Japanese).
Japan Mining Association (1980), "Construction Standards for Tailings Dams", (in Japanese).
Japanese National Committee on Large Dams (1978), "2nd Revised Standards for Dam Design", (in Japanese).
Kusano, K. and Abe H. (1983), "Seismic Analysis of Embankment Considering Liquefaction Ground", Annual Report of Institute of Civil Engineering of Tokyo Metropolitan Government, (in Japanese).
Kutara, K. and Koga, Y. (1975), "A Large Shaking Table Test of Model Embankment", Technical Memorandum of PWRI, NO. 1032, (in Japanese).
Seed, H.B. (1966), "A Method for Earthquake Resistant Design of Earth Dams", Jour. of SMFD, Proc. ASCE, Vol. 92, No. SM1.
Seed, H.B. (1979), "Considerations in the Earthquake Resistant Design of Earth and Rockfill Dams", Geotechnique 29, no. 3.
Uezawa, H. et al (1972), "Experimental Study on Aseismicity of Embankment by Use of Large Shaking Table", Railway Technical Research Report, No. 822, Railway Technical Research Institute, Japanese National Railways, (in Japanese).